

UCSF

UC San Francisco Previously Published Works

Title

An accelerated PETALUTE MRI sequence for in vivo quantification of sodium content in human articular cartilage at 3T.

Permalink

<https://escholarship.org/uc/item/8mq6597b>

Journal

Skeletal Radiology, 54(3)

Authors

Villarreal, Cameron

Shen, Xin

Alhulail, Ahmad

et al.

Publication Date

2025-03-01


DOI

10.1007/s00256-024-04774-5

Peer reviewed



An accelerated PETALUTE MRI sequence for in vivo quantification of sodium content in human articular cartilage at 3T

Cameron X. Villarreal¹ · Xin Shen^{1,2} · Ahmad A. Alhulail³ · Nicholas M. Buffo¹ · Xiaopeng Zhou⁴ · Evan Pogue⁴ · Ali Caglar Özen⁵ · Mark Chiew^{6,7,8} · Stephen Sawiak⁹ · Uzay Emir^{4,10} · Deva D. Chan^{1,11} 

Received: 15 May 2024 / Revised: 9 August 2024 / Accepted: 11 August 2024 / Published online: 17 August 2024
© The Author(s) 2024

Abstract

Objective In this work, we evaluate the sodium magnetic resonance imaging (MRI) capabilities of a three-dimensional (3D) dual-echo ultrashort echo time (UTE) sequence with a novel rosette petal trajectory (PETALUTE), in comparison to the 3D density-adapted (DA) radial spokes UTE sequence in human articular cartilage in the knee.

Materials and methods We scanned five healthy subjects using a 3D dual-echo PETALUTE acquisition and two comparable implementations of 3D DA-radial spokes acquisitions, one matching the number of k-space projections (Radial – Matched Spokes) and the other matching the total number of samples (Radial – Matched Samples) acquired in k-space.

Results The PETALUTE acquisition enabled equivalent sodium quantification in articular cartilage volumes of interest (168.8 ± 29.9 mM, mean \pm standard deviation) to those derived from the 3D radial acquisitions (171.62 ± 28.7 mM and 149.8 ± 22.2 mM, respectively). We achieved a 41% shorter scan time of 2:06 for 3D PETALUTE, compared to 3:36 for 3D radial acquisitions. We also evaluated the feasibility of further acceleration of the PETALUTE sequence through retrospective compressed sensing with $2\times$ and $4\times$ acceleration of the first echo and showed structural similarity of 0.89 ± 0.03 and 0.87 ± 0.03 when compared to non-retrospectively accelerated reconstruction.

Conclusion We demonstrate improved scan time with equivalent performance using a 3D dual-echo PETALUTE sequence compared to the 3D DA-radial sequence for sodium MRI of articular cartilage.

Keywords Sodium MRI · Ultrashort echo time · Fixed charge density · Articular cartilage

✉ Deva D. Chan
chand@purdue.edu

¹ Weldon School of Biomedical Engineering, Purdue University, West Lafayette, IN 47907, USA

² Radiology and Biomedical Imaging, University of California San Francisco, San Francisco, CA 94158, USA

³ Department of Radiology and Medical Imaging, Prince Sattam Bin Abdulaziz University, 16278 Al-Kharj, Saudi Arabia

⁴ College of Health and Human Sciences, Purdue University, West Lafayette, IN 47907, USA

⁵ Division of Medical Physics, Department of Diagnostic and Interventional Radiology, Faculty of Medicine, University Medical Center Freiburg, University of Freiburg, Freiburg, Germany

⁶ Department of Medical Biophysics, University of Toronto, Toronto, Canada

⁷ Physical Sciences, Sunnybrook Research Institute, Toronto, Canada

⁸ Nuffield Department of Clinical Neurosciences, University of Oxford, Oxford, UK

⁹ Department of Physiology, Development, and Neuroscience, University of Cambridge, Cambridge, UK

¹⁰ Department of Radiology, School of Medicine, University of North Carolina, Chapel Hill, NC 27599, USA

¹¹ School of Mechanical Engineering, Purdue University, West Lafayette, IN 47907, USA

Introduction

Loss of glycosaminoglycan (GAG) from articular cartilage is an early hallmark of osteoarthritis [1–3]. GAGs, which are negatively charged, result in high cartilage fixed charge density, which is balanced by cations in the interstitial fluid. Sodium (^{23}Na) magnetic resonance imaging (MRI) signal can be used as a direct measure of GAG content [4, 5], through its direct relationship with maintaining the charge balance against the negative tissue fixed charge density [6]. Therefore, ^{23}Na MRI could provide valuable diagnostic information during the early stages of osteoarthritis progression before the onset of pain or radiographic joint space narrowing, as quantified by the Kellgren-Lawrence grading scale [7]. Despite the potential of ^{23}Na MRI as a powerful diagnostic tool for early osteoarthritis, its practical use in the clinic is hampered by long scan times, poor spatial resolution, and low inherent sodium content, which typically prompts the need for higher magnetic field strength [8, 9]. Additionally, the physical properties of sodium (i.e., 3/2 spin quadrupolar interaction, fast T_2 relaxation, gyromagnetic ratio [10]) and its lower abundance lead to reduced sensitivity and a correspondingly low signal-to-noise ratio (SNR) [11], making it necessary to use an ultrashort echo time (UTE) sequence. The low thickness of articular cartilage in healthy adult humans [12] also presents a challenge for sodium MRI, since high spatial resolution and therefore longer scan times are preferred for both avoiding partial volume effects and measuring spatially varying sodium signal in cartilage.

Advancements in UTE sequences have enabled better imaging and quantification of sodium *in vivo*. UTE sequences enable adequate coverage of k-space before substantial decay of the signal (T_2^* of 13.2 ms [13]), although the trajectories with which they traverse k-space differ. Some common 3D trajectories include cones, spiral, and density-adapted (DA) radial spokes [9, 13, 14]. Currently, the 3D radial acquisition is often employed for sodium imaging in cartilage due to its ability to rapidly acquire signal at high resolution with relatively short echo time. This results in a high-quality sodium signal without sacrificing acquisition time. The 3D radial acquisition has also been used for *in vivo* quantifying sodium concentration in cartilage at 3 T and 7 T. Recently, Shen, et al., developed a novel 3D rosette petal trajectory UTE (PETALUTE) sequence that features a curvilinear, petal-like trajectory, in contrast to the linear trajectory of a radial spoke [15]. Using proton MRI of the brain, they showed that 3D dual-echo PETALUTE trajectory achieved comparable coverage of k-space and signal quality as 3D radial at a shorter total acquisition time [15].

In this work, our objective was to evaluate the PETALUTE sequence for *in vivo* sodium MRI of the human knee

and sodium content quantification in articular cartilage. Toward the goal of addressing several limitations to sodium MRI, we demonstrate that the 3D dual-echo rosette acquisition reduces scan time while preserving signal quality when compared to the 3D DA-radial spokes acquisition. Furthermore, we demonstrate the ability to further accelerate the PETALUTE acquisition via compressed sensing without a significant reduction in signal quality.

Methods

3D dual-echo UTE MRI with novel rosette k-space trajectory (PETALUTE)

We implemented a novel rosette trajectory for a 3D UTE acquisition that traverses k-space with multiple crossings of the k-space origin (Fig. 1) [15]. Briefly, the petal-like sampling enabled a dual-echo acquisition, with petal trajectory passing through the k-space center at the start and end of each repetition. Crusher gradients were applied in all three directions at the end of each readout gradient. Images were reconstructed from the first and second half of each petal. Two hundred ten samples per petal and 18,050 petals are acquired with an acceleration factor of 2. Due to the efficient sampling of the novel rosette k-space pattern, only 80% of the required k-space (a total of 31,600 samples) can be considered full-k-space acquisition [15].

Subject selection and scan parameters

Under Institutional Review Board approval, we scanned the right knees of five healthy volunteers (29.6 (mean) \pm 13.4 (standard deviation) years old, 1 female) in a Siemens MAGNETOM Prisma 3-Tesla MRI scanner (Siemens Healthineers, Germany). We positioned each subject supine and foot first and used a goniometer to flex the knee at 15° before adding foam padding and securing the dedicated knee coil. With the joint midline (identified via palpation) aligned to the isocenter, ^1H anatomical reference scans were acquired using the integrated body coil to mitigate registration error between proton and sodium images. All volunteers self-reported no history of joint trauma or disease and showed no indications of musculoskeletal disease on anatomical scans.

Using a frequency-tuned, mono-resonant ^{23}Na transmit-receive knee volume coil (32.6 MHz, Stark-Contrast, Erlangen, Germany), we compared the 3D dual-echo rosette sequence [15] to two implementations of the 3D DA-radial spokes sequence (Table 1). We adjusted the radial sequence to either match the same number of points sampled in k-space (“Radial – Matched Samples”) or the same number of projections into k-space (“Radial

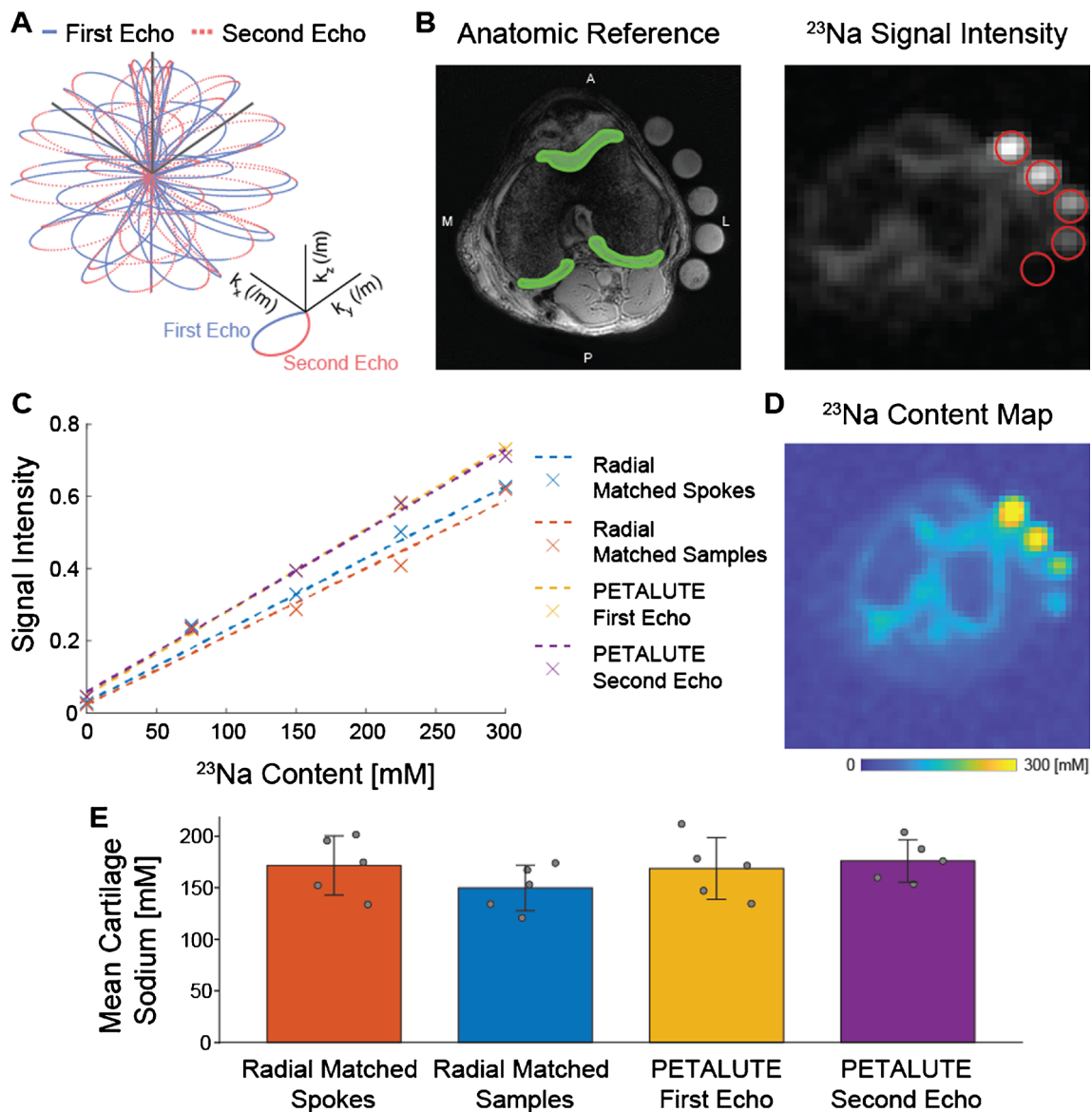


Fig. 1 Dual-echo PETALUTE was compared to Radial UTE for 3D acquisition of sodium quantification in articular cartilage. **A** 3D dual-echo PETALUTE is a novel k-space trajectory that enables more efficient sampling of the edges of k-space. The outward (solid blue) and inward (dashed red) petal-like trajectories enable the acquisition of dual-echo images. **B** Cartilage regions of interest (green sections) were manually segmented using the anatomical reference for each subject. Subjects and sodium concentration standards (red cir-

cles) were scanned with 3 different sodium MRI acquisitions: 3D dual-echo PETALUTE (representative axial slice shown), Radial – Matched Samples, and Radial – Matched Spokes. **C** A linear curve fit was used to calibrate sodium signal intensity. **D** Signal intensity was then converted to sodium concentration maps. **E** Sodium concentrations were averaged over the cartilage ROIs for each subject and UTE acquisition, with mean \pm standard deviation concentrations also shown

– Matched Spokes”). Comparisons to DA-radial acquisitions were performed against one of two images acquired with the 3D rosette dual-echo sequence (“Rosette – First Echo,” “Rosette – Second Echo”). The lowest possible repetition time (TR) and echo time (TE) were chosen for each sequence.

Sodium concentration standards

We prepared sodium phantoms using NaCl (0, 75, 150, 225, 300 mM) and 10% agarose w/v in distilled water in 15 mL conical tubes to generate a series of concentration standards that encompass the expected physiological range of sodium

Table 1 Acquisition parameters for each of the UTE sequences compared in the study

UTE sequence parameters	Dual-echo rosette (PETALUTE)	Radial – Matched Samples	Radial – Matched Spokes
Number of averages (NA)	3	3	3
Repetition time (TR)	7 ms	12 ms	12 ms
Number of PETAL/spokes	18,050	18,050	18,050
Number of points sampled per petals/spokes	218	256	384
RF pulse duration	100 μ s	500 μ s	500 μ s
ADC bandwidth	100 kHz	25 kHz	38 kHz
Echo time (TE)	90 μ s, 2270 μ s	300 μ s	300 μ s
3D field of view (FOV)	360 mm	320 mm	320 mm
Ernst angle	44°	55°	55°
Acquisition time (mm:ss)	2:06	3:36	3:36

which has been measured up to ~280 mM within healthy human femoral cartilage [6, 16]. We secured the phantoms to the lateral aspect of each subject's knee for scanning, and they were included in the field of view during all scans.

Image reconstruction and sequence comparisons

We reconstructed images via regular regridding applying a density-compensated adjoint nonuniform fast Fourier transform using the BART toolbox [17] in MATLAB (MathWorks, USA). We used a non-uniform fast Fourier transform (NUFFT) [18] to calculate the forward-encoding transform of the acquired k-space information acquired with the rosette UTE sequence [19]. For PETALUTE acquisitions, a compressed sensing approach was used for image reconstruction using total generalized variation as the sparsifying penalty [18, 20]. For both PETALUTE (acceleration factor of 2) and DA-radial, we applied a Hanning filter for regular regridding, density-compensated adjoint NUFFT. The resulting reconstructions resulted in a nominal resolution of 2.81 mm (isotropic). We determined the signal-to-noise ratio by dividing the average signal intensity value in cartilage regions of interest by the mean signal intensity of the phantom with 0 mM sodium concentration, which should be associated with noise in a sodium MRI acquisition.

Sodium quantification

To calibrate sodium concentration to acquired signal intensity, we identified the regions occupied by our sodium concentration standards, quantified the mean intensity value

within each using five representative slices, and performed a linear curve fit to obtain a standard curve for each acquisition. Using this linear relationship, we performed voxel-wise sodium signal-to-concentration conversion. We manually segmented cartilage using anatomical reference scans and used these regions of interest to quantify the sodium concentration within cartilage (Fig. 1).

Retrospective compressed sensing

To demonstrate further capabilities to decrease scan time, we applied compressed sensing of rosette acquisitions retrospectively using acceleration factors of 2 \times and 4 \times by pseudo-random under-sampling of k-space. We pseudo-randomly utilized one-half and one-quarter of the petals to reconstruct dual-echo images using the same reconstruction pipeline described previously. These simulated data sets were compared to dual-echo images with no acceleration factor using a structural similarity (SSIM) coefficient (*ssim* function, MATLAB, MathWorks). For each subject, we compared a cuboid volume of interest that contained the knee and determined the mean SSIM coefficient across all subjects.

Statistical analysis

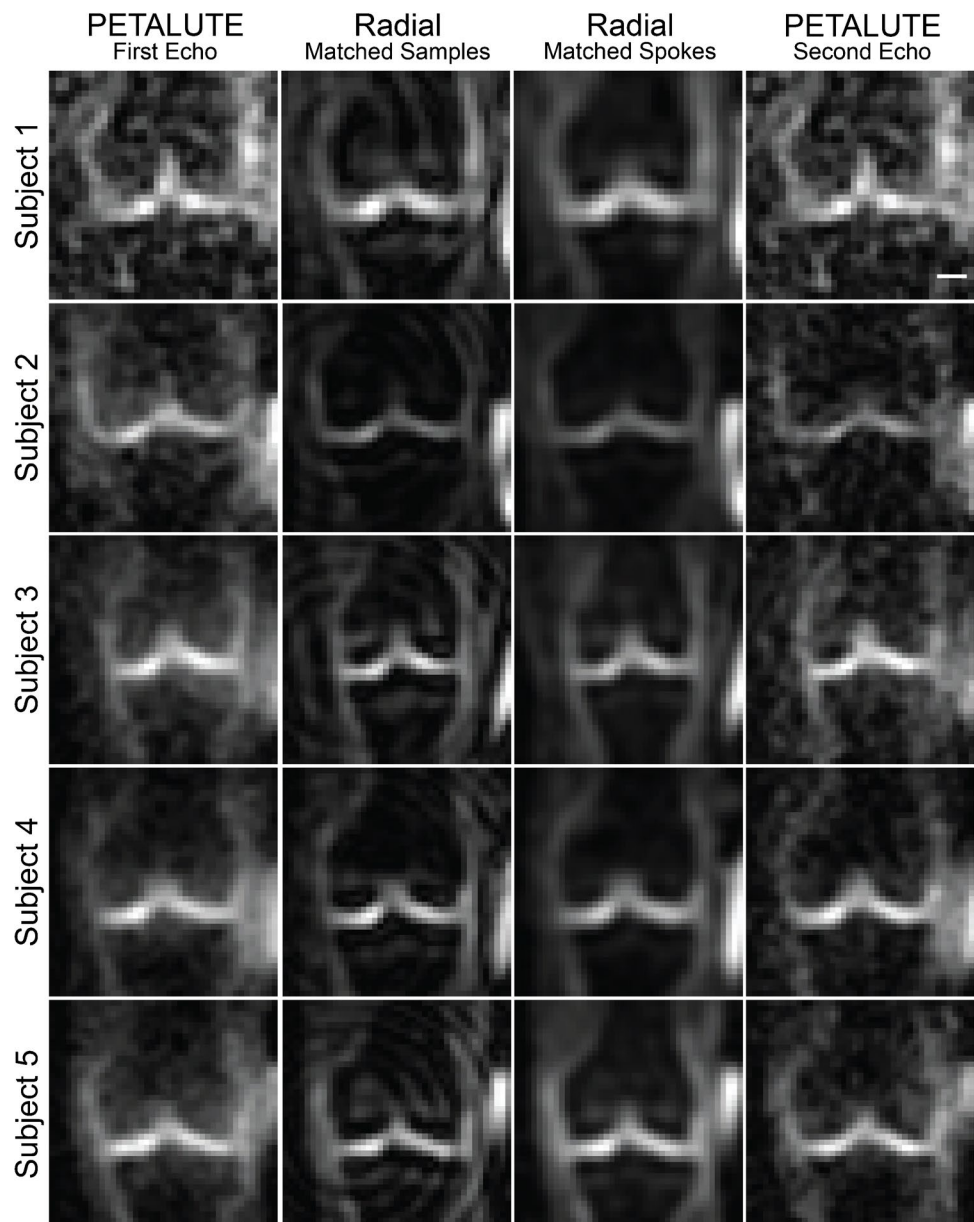
All results are reported as mean \pm standard deviation. We compared mean sodium concentrations using a Kruskal–Wallis test and evaluated the agreement between cartilage sodium concentration using a Bland–Altman test, comparing pixel-wise within each subject and as averaged values for cartilage in each subject. We used the PETALUTE – First Echo as our reference (all difference values were obtained by subtracting the sodium signal of each acquisition from the PETALUTE – First Echo values). The limits of agreement represent a 95% confidence interval centered on the mean difference for each comparison. Statistical analyses were performed in Rstudio [21], a development environment for R [22], using native functions and the *blandr* package [23].

Results

Sequence comparisons

Dual-echo PETALUTE and DA-radial acquisitions (matched by samples and by number of spokes) were used for sodium MRI of the knee in 5 human volunteers (Fig. 2). The Radial Matched-Samples acquisition produced a ringing artifact in all subjects that was not observed in either of reconstruction for the dual-echo PETALUTE sequence or Radial Matched-Spokes acquisition. Calibration using sodium standards enabled the calculation of sodium content maps (Fig. 3). For

Fig. 2 ^{23}Na MRI of the knee was implemented using PETALUTE and DA-Radial UTE. Cuboid cropped volumes were centered on the joint midline and include the distal femur and proximal tibia. Coronal slices centered on the joint space are shown for each subject and UTE acquisition. Scale bar = 1.5 cm



the same number of averages, PETALUTE allowed us to achieve a 41% reduction in total scan time. The SNR in knee cartilage was determined to be 9.2 ± 3.2 and 8.2 ± 2.9 for the first echo of the PETALUTE and Radial-Matched Spokes, respectively ($p=0.62$).

Sodium quantification

We calculated mean sodium values within cartilage of 173.0 ± 27.4 mM for PETALUTE– First Echo, 180.2 ± 34.3 mM for Radial – Matched Spokes, 146.7 ± 21.6 mM, and for Radial – Matched Samples (Fig. 1). Sodium concentration maps were derived from PETALUTE acquisition from which we subtracted the Radial UTE acquisitions to determine

spatially dependent differences in the acquisitions (Fig. 4A). The mean differences in measured cartilage sodium content between PETALUTE– First Echo and Radial – Matched Samples and Radial – Matched Spokes were 26.34 ± 15.67 mM and -7.146 ± 29.8 mM, respectively, and were not statistically significant ($p=0.199$ and $p=0.668$, respectively). The difference in measured sodium concentration between the first and second echo of PETALUTE was 12.99 ± 16.65 mM, which was not statistically significant ($p=0.656$). The Bland–Altman mean-difference test showed that the limits of agreement for sodium concentration between each of the sequences bounded zero for pixel-wise comparisons within each subject (Supplemental Fig. 1) and for mean cartilage sodium content across all subjects (Fig. 4B).

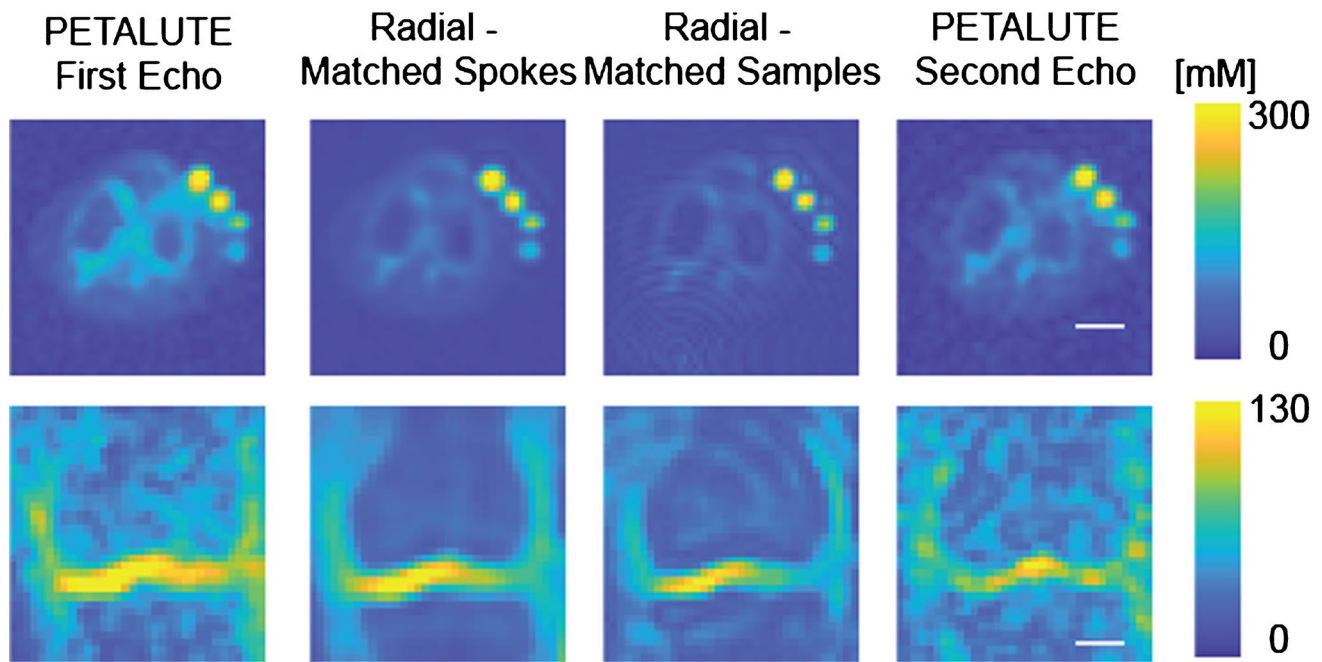


Fig. 3 Sodium maps derived from dual-echo PETALUTE and Radial UTE were compared. Representative sodium maps are shown for a single subject for each of the UTE acquisitions. The axial images are cropped to 14.05 cm × 14.05 cm so that all phantoms and the knee are in view. Separately, a coronal slice, cropped to 11.2 cm × 11.2 cm of

the same subject, is shown, focusing on visualization of the tibial and femoral cartilage for medial and lateral compartments, allowing for a color range that is not dominated by the sodium phantom signal. Scale bar = 2.5 cm

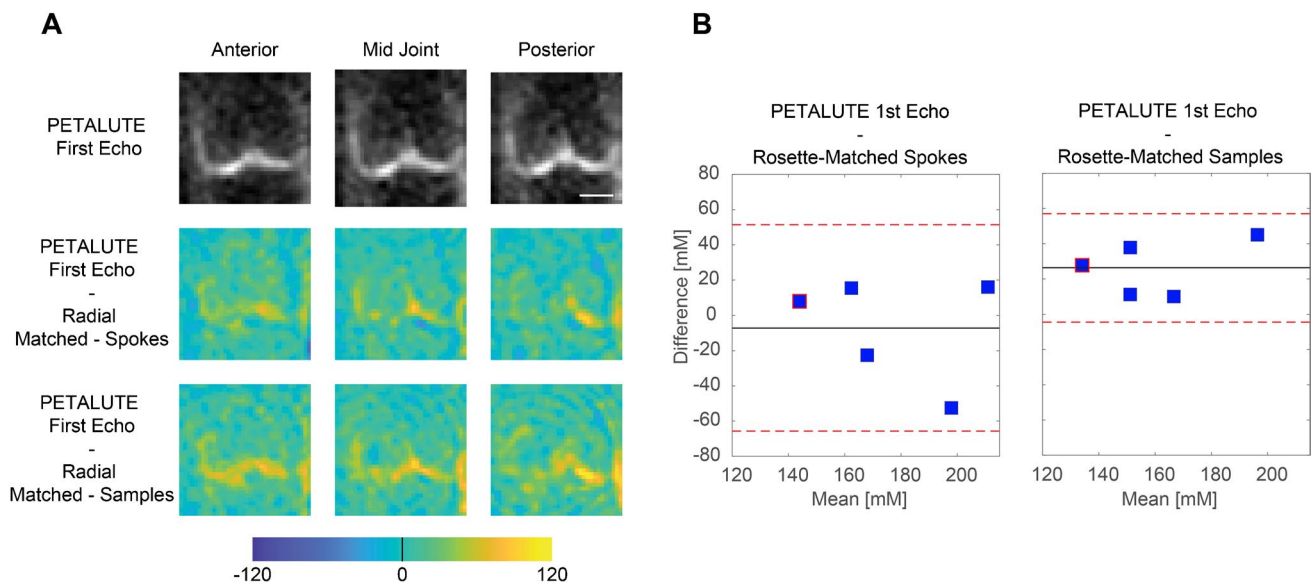


Fig. 4 Sodium quantification with the PETALUTE and radial acquisitions shows strong agreement. The PETALUTE and radial acquisitions perform similarly for sodium content quantification. **A** Differences in sodium measurements were calculated by subtracting the sodium maps, derived from a radial acquisition, from the sodium map derived from the PETALUTE – First Echo acquisition. Three images from a representative subject are shown, the first and last slices (anteriorly and posteriorly) in which femoral cartilage is present and the center of the joint. The reference PETALUTE – First Echo acquisition is shown in the first row of images. **B** The Bland–Altman test

was performed to determine the limits of agreement between each combination of sequences, using PETALUTE – First Echo as the reference. Limits of agreement are denoted by red dashed horizontal lines, while the mean difference is denoted by a solid black line. For each subject, the mean and difference in sodium concentration in knee cartilage are plotted for the comparisons between PETALUTE – First Echo and Radial – Matched Spokes Samples and Radial – Matched Samples. The data points for the representative subject are indicated in red on these plots

Retrospective compressed sensing

We retrospectively evaluated imaging acceleration by down-sampling unaccelerated acquisitions prior to compressed sensing reconstruction. Using unaccelerated PETALUTE – First Echo as the reference, SSIM indices were found to be 0.93 ± 0.02 and 0.89 ± 0.03 for $2\times$ and $4\times$ acceleration factors, respectively. For PETALUTE – Second Echo, SSIM indices were 0.90 ± 0.02 and 0.87 ± 0.03 , respectively (Fig. 5).

Discussion

In this study, we demonstrate for the first time a 3D dual-echo novel rosette acquisition, PETALUTE [15], for sodium UTE MRI of the human knee. Using 3D PETALUTE, we achieved a rapid acquisition of sodium signal with a high agreement in sodium quantification in articular cartilage with the 3D radial acquisition, with a 41% improvement in total acquisition time (Table 1). Additionally, we demonstrated the potential for even shorter acquisition via acceleration of $2\times$ and $4\times$ through a simulated compressed sensing acquisition and showed high structural similarity to the non-accelerated, full k-space rosette acquisition. Our results demonstrate that the novel 3D dual-echo rosette sequence [15] can rapidly acquire sodium signal with a high degree of

agreement with the radial spokes acquisition and at a faster total scan time.

To demonstrate the application of PETALUTE for sodium MRI of the knee, we compared the 3D dual-echo PETALUTE sequence to the 3D DA-radial spokes sequence. The radial spokes acquisition is commonly used in musculoskeletal imaging [8] and has been well documented for in vivo sodium imaging, particularly in imaging knee cartilage as in this work. For example, Madelin et al. performed 3D radial MRI at 7 T in human knee cartilage [24] which enabled sodium quantification in vivo, but even with 7 T field strength, scan times exceeded 16:50. The 3D radial acquisition has also been used at 3 T to quantify sodium content in the knee [25], but a total acquisition time of 57:45 was required to achieve a 3-mm isometric voxel size with one average. Across all subjects, the Radial – Matched Samples acquisition displayed a pronounced ringing artifact that was not evident in either Radial – Matched Spokes or PETALUTE (Fig. 1), an effect likely attributable to undersampling. On the other hand, the rosette trajectory of PETALUTE provides improved k-space coverage which enables undersampling without losing image quality [15, 26]. Because of this improved efficiency, PETALUTE enabled an appreciably shorter total scan time of 2:06 (min:sec) compared to 3:36 while not significantly affecting sodium concentration measurements (Fig. 1). In addition, a dual-echo acquisition was possible even with the reduced scan

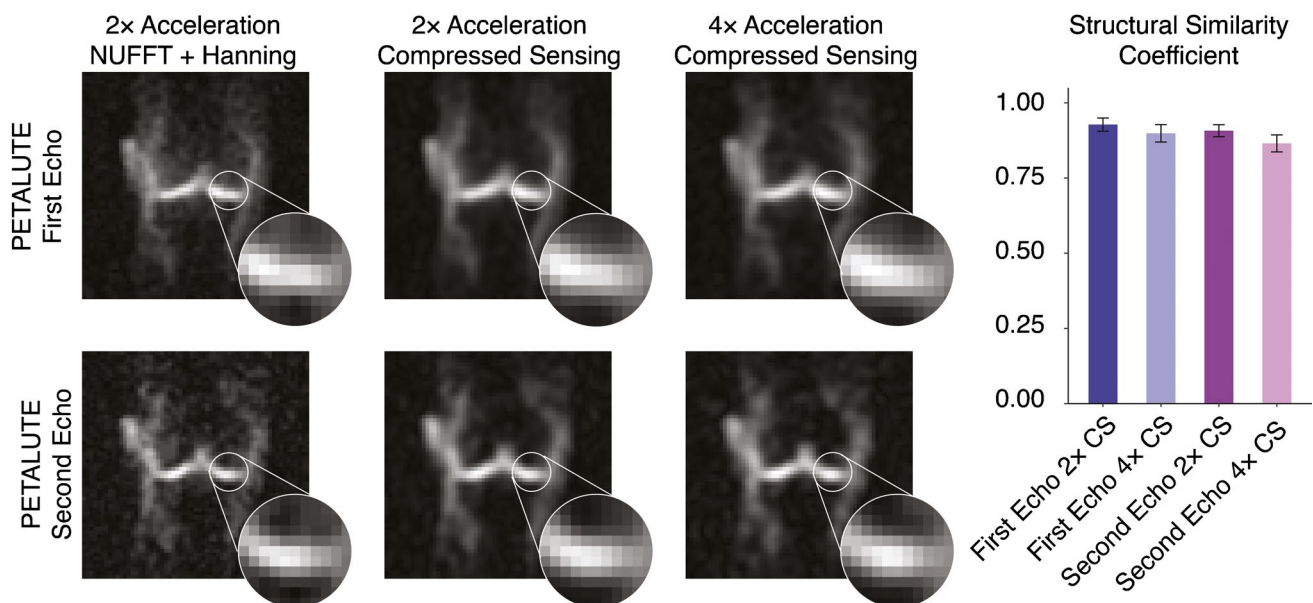


Fig. 5 Retrospective compressed sensing demonstrates the capability for at least four times acceleration while preserving the image quality of dual-echo PETALUTE acquisitions. **A** Retrospective down-sampling of unaccelerated PETALUTE acquisitions was used to evaluate $2\times$ and $4\times$ acceleration via compressed sensing. **B** Structural similar-

ity indices were calculated for each subject, and both echoes showed high agreement with unaccelerated images. Qualitatively, boundaries between regions of high and low sodium signal intensity retain their similarity even at higher levels of acceleration

time, compared to a single radial UTE echo. Although our comparison here has focused only on the first echo, the second echo—as well as additional echoes—could be used for sodium T_2^* quantification, providing yet another metric to evaluate cartilage in future applications of PETALUTE. This second echo could also be combined with the first echo to further improve signal quality [27] but without the need for an additional scan.

We achieved comparable SNR with PETALUTE at 2.81-mm nominal resolution despite the shorter total scan time, with a mean SNR in knee cartilage of 9.2 using the first echo of PETALUTE and 8.2 for Radial – Matched Spokes. Achieving high SNR improves the accuracy of tissue sodium concentration quantification, while increased resolution enables finer details to be captured, a point of particular importance with thin tissues like cartilage. Although direct comparisons of SNR cannot be made without matching all image parameters on the same system in the same subjects, increased averaging and resolution with PETALUTE—potentially in combination with compressed sensing—could readily match the SNR of previously reported studies. Other studies have reported an SNR of 30 in knee cartilage for the 3D radial sequence with 2-mm nominal isotropic resolution at 3 T with a total acquisition time of 20 min [28]. In another study, 3D cones achieved an SNR of 11.3 in patellar cartilage with $1.3 \times 1.3 \times 4 \text{ mm}^3$ resolution at 3 T with a total scan time of 25:50 [13]. A 7T study employed a 17-min 3D radial acquisition, at a nominal resolution of 2-mm isotropic, for an SNR of 43.8 ± 7.5 in patellar cartilage [29]. Since SNR is directly proportional to field strength and the square root of the number of averages, PETALUTE using the parameters in this 3T study with 8 averages (matching total acquisition time of about 17 min) would be expected to exceed the SNR (~ 60 , compared to 43.8 [29]). Furthermore, we showed that PETALUTE performs with high structural similarity even with acceleration by compressed sensing (Fig. 5), enabling further reductions in total scan time. Additionally, an even shorter acquisition is possible by removing the crusher gradients [26].

Beyond total scan time and SNR, PETALUTE also performed as well as the 3D DA-radial UTE sequence for quantifying sodium signal in articular cartilage in vivo. Using PETALUTE acquisition, we found no statistical difference ($p = 0.345$) in the sodium concentration quantified from the Radial – Matched Spokes acquisition (Fig. 1), a well-established method for in vivo cartilage sodium quantification [25]. A Bland–Altman test showed limits of agreement that bounded zero and indicated a small, statistically insignificant difference in mean sodium content between the PETALUTE and radial UTE acquisitions.

These findings illustrate the capabilities of the novel 3D dual-echo rosette sequence to match the performance of the 3D radial acquisition while improving scan time,

addressing one of the critical barriers to clinical translation of sodium MRI. However, all sequences tested in our study resulted in estimated sodium concentrations below the expected in vivo sodium concentration of cartilage. Other works, which reported similarly unexpectedly low signal in healthy tissue, attributed this effect to the high water content ($\sim 75\%$ total weight) of cartilage [28, 30]. Accordingly, a correction factor of $1/0.75$ has been proposed for cartilage to account for this sodium signal attenuation [24]. The average sodium concentration would have fallen within the expected physiological range for all acquisitions if we had adjusted concentrations by the correction factor. However, it is important to note that as the water content in the cartilage changes with the loss of GAG during early osteoarthritis [31], a constant calibration factor may not be appropriate in diagnostic practice.

Interestingly, we noted qualitative differences in image quality and sodium concentration mapping between the PETALUTE and the radial spokes acquisitions, although these could be attributed to the sampling approach in the Radial – Matched Samples acquisition. This approach used the same number of points sampled in k-space compared to PETALUTE, but due to the trajectory of the radial spokes, this resulted in sampling near the Nyquist frequency. Additionally, we noted a difference in the sodium signal distribution in articular cartilage, particularly in the outer regions of the knee, between PETALUTE and radial UTE. In the sodium content difference images (Fig. 4), higher sodium content is measured at mid-joint with PETALUTE than Radial – Matched Spokes. Additionally, we observed that the interfaces between tissue (ie: cartilage to bone), and the medial regions of femoral cartilage, tend to be sites of greater magnitude of sodium signal difference (Fig. 4). With the radial acquisitions, the sodium signal intensity appeared to attenuate with distance from the center of the knee. However, in healthy articular cartilage, PG content, and thus the fixed charge density and sodium distribution, is not expected to differ substantially by location in the joint [32]. In contrast, the PETALUTE acquisition showed similar sodium signal intensity in the inner and outer regions of the joint, suggesting no signal drop-off further from the center of the joint. Similarly, with retrospective compressed sensing, there was no qualitative difference in the signal pattern at the cartilage margins in any of the retrospective accelerations compared to the unaccelerated scans (Fig. 5). The sharp signal gradients at the cartilage margins were preserved, even under $4 \times$ acceleration, for both echoes, suggesting minimal loss of high-frequency information. This could be due to the greater density of sampling of outer k-space [33] where finer details, sharp transitions, and other higher frequency information are located.

Although we demonstrate that PETALUTE performs comparably to radial UTE for cartilage sodium quantification

at a reduced scan time, there are limitations inherent to such a comparison study. The scan times demonstrated here are up to an order of magnitude lower than typical sodium UTE studies, even for radial UTE, because we targeted reduced scan time to address a major barrier to clinical use. We optimized for short PETALUTE imaging times in this comparison and tuned the radial UTE sequence to achieve the same coverage at comparable times. This also enabled us to minimize motion between long scans in our volunteers, noting the 20+ min scan times of a conventional sodium UTE study [13, 28], while pushing the technical limits on reducing scan time. Given that we optimized for fast imaging time in this study, future stand-alone applications of PETALUTE for cartilage sodium quantification can instead optimize for finer resolution and greater SNR at the cost of total imaging time. Additionally, measurement of sodium concentration in thin tissues such as cartilage is sensitive to partial volume effects, especially with the coarse resolution of typical sodium UTE scans. However, the same volume of interest was used in all comparisons here and thus partial volume effects would be equivalent across comparisons. Utilizing an anatomic reference scan in an iterative reconstruction approach [34] or similar image processing method could also improve the resolution of a PETALUTE acquisition.

In conclusion, we have demonstrated PETALUTE, a novel 3D rosette k-space trajectory, for sodium MRI of articular cartilage. Sodium MRI has the potential to become a powerful early diagnostic tool in cartilage degeneration, but its clinical translation is hindered by several factors, including long scan times and poor spatial resolution. In this work, we showed reduced scan time with PETALUTE compared to comparable radial acquisitions with a high degree of agreement in sodium quantification. Using retrospective analyses, we also demonstrated the potential for greater acceleration of PETALUTE for sodium MRI through compressed sensing. Sodium MRI with 3D dual-echo PETALUTE acquisition, therefore, addresses several of the current barriers to clinical translation of sodium quantification in healthy and degenerating articular cartilage.

Supplementary Information The online version contains supplementary material available at <https://doi.org/10.1007/s00256-024-04774-5>.

Acknowledgements We thank Armin M. Nagel for providing the radial sequence for comparison.

Funding Data acquisition was supported in part by NIH grant S10 OD012336. In addition, D.D.C. was supported in part by NSF grant 2149946, and C.X.V. was supported in part by NIH training grant T32 DK101001.

Declarations

Ethics approval and consent to participate All procedures performed in studies involving human participants were in accordance with the ethical standards of the institutional and/or national research commit-

tee and with the 1964 Helsinki Declaration and its later amendments or comparable ethical standards. Informed consent was obtained from all individual participants in the study, including permission to report identifying information, including images, in this article.

Conflict of interest The authors declare no competing interests.

Open Access This article is licensed under a Creative Commons Attribution 4.0 International License, which permits use, sharing, adaptation, distribution and reproduction in any medium or format, as long as you give appropriate credit to the original author(s) and the source, provide a link to the Creative Commons licence, and indicate if changes were made. The images or other third party material in this article are included in the article's Creative Commons licence, unless indicated otherwise in a credit line to the material. If material is not included in the article's Creative Commons licence and your intended use is not permitted by statutory regulation or exceeds the permitted use, you will need to obtain permission directly from the copyright holder. To view a copy of this licence, visit <http://creativecommons.org/licenses/by/4.0/>.

References

1. Mankin HJ, Lippiello L. The glycosaminoglycans of normal and arthritic cartilage. *J Clin Invest*. 1971;50(8):1712–9.
2. Altman RD, Pita JC, Howell DS. Degradation of proteoglycans in human osteoarthritic cartilage. *Arthritis Rheum*. 1973;16(2):179–85.
3. Xia B, Di C, Zhang J, Hu S, Jin H, Tong P. Osteoarthritis pathogenesis: a review of molecular mechanisms. *Calcif Tissue Int*. 2014;95(6):495–505.
4. Lesperance LM, Gray ML, Burstein D. Determination of fixed charge density in cartilage using nuclear magnetic resonance. *J Orthop Res*. 1992;10(1):1–13.
5. Duvvuri U, Kaufman JH, Patel SD, Bolinger L, Kneeland JB, Leigh JS, et al. Sodium multiple quantum spectroscopy of articular cartilage: effects of mechanical compression. *Magn Reson Med*. 1998;40(3):370–5.
6. Shapiro EM, Borthakur A, Dandora R, Kriss A, Leigh JS, Reddy R. Sodium visibility and quantitation in intact bovine articular cartilage using high field (23)Na MRI and MRS. *J Magn Reson*. 2000;142(1):24–31.
7. Kellgren JH, Lawrence JS. Radiological assessment of osteoarthritis. *Ann Rheum Dis*. 1957;16(4):494–502.
8. Bangerter NK, Tarbox GJ, Taylor MD, Kaggie JD. Quantitative sodium magnetic resonance imaging of cartilage, muscle, and tendon. *Quant Imaging Med Surg*. 2016;6(6):699–714.
9. Zbyn S, Mlynarik V, Juras V, Szomolanyi P, Trattnig S. Sodium MR imaging of articular cartilage pathologies. *Curr Radiol Rep*. 2014;2(4):41.
10. Reddy R, Li S, Noyszewski EA, Kneeland JB, Leigh JS. In vivo sodium multiple quantum spectroscopy of human articular cartilage. *Magn Reson Med*. 1997;38(2):207–14.
11. Madelin G, Regatte RR. Biomedical applications of sodium MRI in vivo. *J Magn Reson Imaging*. 2013;38(3):511–29.
12. Sophia Fox AJ, Bedi A, Rodeo SA. The basic science of articular cartilage: structure, composition, and function. *Sports Health*. 2009;1(6):461–8.
13. Staroswiecki E, Bangerter NK, Gurney PT, Grafendorfer T, Gold GE, Hargreaves BA. In vivo sodium imaging of human patellar cartilage with a 3D cones sequence at 3 T and 7 T. *J Magn Reson Imaging*. 2010;32(2):446–51.

14. Nagel AM, Laun FB, Weber MA, Matthies C, Semmler W, Schad LR. Sodium MRI using a density-adapted 3D radial acquisition technique. *Magn Reson Med*. 2009;62(6):1565–73.
15. Shen X, Ozen AC, Sunjar A, Ilbey S, Sawiak S, Shi R, et al. Ultra-short T(2) components imaging of the whole brain using 3D dual-echo UTE MRI with rosette k-space pattern. *Magn Reson Med*. 2023;89(2):508–21.
16. Moon CH, Kim JH, Zhao T, Bae KT. Quantitative (23) Na MRI of human knee cartilage using dual-tuned (1) H/(23) Na transceiver array radiofrequency coil at 7 Tesla. *J Magn Reson Imaging*. 2013;38(5):1063–72.
17. Blumenthal M, Heide M, Holme C, Juschitz M, Rapp B, Schaten P, et al. BART: toolbox for computational magnetic resonance imaging. 2023.
18. Knoll F, Bredies K, Pock T, Stollberger R. Second order total generalized variation (TGV) for MRI. *Magn Reson Med*. 2011;65(2):480–91.
19. Sutton BP, Noll DC, Fessler JA. Fast, iterative image reconstruction for MRI in the presence of field inhomogeneities. *IEEE Trans Med Imaging*. 2003;22(2):178–88.
20. Lustig M, Donoho D, Pauly JM. Sparse MRI: the application of compressed sensing for rapid MR imaging. *Magn Reson Med*. 2007;58(6):1182–95.
21. RStudio Team. RStudio: integrated Development for R. Boston, MA: RStudio, PBC 2020.
22. R Development Core Team. R: a language and environment for statistical computing. Vienna, Austria: R Foundation for Statistical Computing 2010.
23. Datta D. blandr: a Bland-Altman method comparison package for R. 2017.
24. Madelin G, Lee JS, Inati S, Jerschow A, Regatte RR. Sodium inversion recovery MRI of the knee joint in vivo at 7T. *J Magn Reson*. 2010;207(1):42–52.
25. Kamp B, Frenken M, Henke JM, Abrar DB, Nagel AM, Gast LV, et al. Quantification of sodium relaxation times and concentrations as surrogates of proteoglycan content of patellar cartilage at 3T MRI. *Diagnostics (Basel)*. 2021; 11(12).
26. Shen X, Caverzasi E, Yang Y, Liu X, Green A, Henry RG, et al. 3D balanced SSFP UTE MRI for multiple contrasts whole brain imaging. *Magn Reson Med*. 2024.
27. Biondetti E, Karsa A, Grussu F, Battiston M, Yiannakas MC, Thomas DL, et al. Multi-echo quantitative susceptibility mapping: how to combine echoes for accuracy and precision at 3 Tesla. *Magn Reson Med*. 2022;88(5):2101–16.
28. Madelin G, Babb JS, Xia D, Chang G, Jerschow A, Regatte RR. Reproducibility and repeatability of quantitative sodium magnetic resonance imaging in vivo in articular cartilage at 3 T and 7 T. *Magn Reson Med*. 2012;68(3):841–9.
29. Madelin G, Chang G, Otazo R, Jerschow A, Regatte RR. Compressed sensing sodium MRI of cartilage at 7T: preliminary study. *J Magn Reson*. 2012;214(1):360–5.
30. Shapiro EM, Borthakur A, Gougoutas A, Reddy R. ²³Na MRI accurately measures fixed charge density in articular cartilage. *Magn Reson Med*. 2002;47(2):284–91.
31. Calvo E, Palacios I, Delgado E, Sanchez-Pernaute O, Largo R, Egido J, et al. Histopathological correlation of cartilage swelling detected by magnetic resonance imaging in early experimental osteoarthritis. *Osteoarthritis Cartilage*. 2004;12(11):878–86.
32. Gurr E, Mohr W, Pallasch G. Proteoglycans from human articular cartilage: the effect of joint location on the structure. *J Clin Chem Clin Biochem*. 1985;23(12):811–9.
33. Shen X, Ozen AC, Monsivais H, Sunjar A, Ilbey S, Zheng W, et al. High-resolution 3D ultra-short echo time MRI with rosette k-space pattern for brain iron content mapping. *J Trace Elem Med Biol*. 2023;77: 127146.
34. Gnahm C, Nagel AM. Anatomically weighted second-order total variation reconstruction of ²³Na MRI using prior information from 1H MRI. *Neuroimage*. 2015;105:452–61.

Publisher's Note Springer Nature remains neutral with regard to jurisdictional claims in published maps and institutional affiliations.